How chiral vibrations drive molecular rotation

How chiral vibrations drive molecular rotation

Ivan Pasqua,[1] Gregorio Staffieri,[1,*] and Michele Fabrizio[1]

[1] *International School for Advanced Studies (SISSA), Via Bonomea 265, I-34136 Trieste, Italy*

We analyze two simple model planar molecules: an ionic molecule with D_3 symmetry and a covalent molecule with D_6 symmetry. Both symmetries allow the existence of chiral molecular orbitals and normal modes that are coupled to each other in a Jahn-Teller manner, invariant under $U(1)$ symmetry with generator a pseudo angular momentum. In the ionic molecule, the chiral mode possesses an electric dipole but lacks physical angular momentum, whereas, in the covalent molecule, the situation is reversed. In spite of that, we show that in both cases the chiral modes can be excited by a circularly polarized light and are subsequently able to induce rotational motion of the entire molecule.

INTRODUCTION

The Einstein-de Haas (EdH) effect [1] and its reciprocal, the Barnett effect [2], were discovered over a century ago, but are currently experiencing a revival of interest [3–8], especially after the prediction [9–11], and possible observation [12] that chiral phonons may play the same role of the electron spins in the original experiments [1, 2], see [13] for a recent review.

While the ultimate explanation of the EdH effect is the conservation of total angular momentum, the precise mechanisms that enable the transfer of the angular momentum carried by microscopic internal degrees of freedom to the macroscopic rigid body rotation are considerably more challenging to elucidate. This stems primarily from the fact that commonly employed model Hamiltonians do not explicitly incorporate global degrees of freedom, such as the sample angle of rotation. Furthermore, the EdH effect caused by the excitations of specific phonon modes encounters an additional challenge. In most cases, these phonons only carry a pseudo angular momentum [14], and it remains unclear how the latter can be converted into a physical angular momentum. It has also been noted [15] that a faithful description of experiments that detect evidence of phonon magnetic moments necessitates degenerate chiral phonons coupled to degenerate electronic orbitals, thereby realizing a form of Jahn-Teller effect that is in fact associated with the conservation of a pseudo angular momentum distinct from the physical one.

Based on these observations, in this work we aim to clarify these questions by introducing and analyzing two toy models that describe two distinct types of planar molecules: an ionic and a covalent one, exemplified by metal trifluoride MF_3 (M=Al, Sc, Y), and by benzene, C_6H_6, respectively. These models possess chiral degenerate normal modes and degenerate molecular orbitals, thereby accurately capturing the physical phenomena discussed above. The choice of ionic and covalent molecules is motivated by their realization of two distinct types of Jahn-Teller coupling.

In the ionic molecule discussed in Sec. I, the Jahn-Teller effect originates from the dependence on the ion displacement of the crystal field experienced by the electrons, and explicitly involves the global angle of rotation of the molecule, as shown in Sec. I B. Although this aspect is often overlooked, it is crucial for understanding how the pseudo-angular momentum associated with the Jahn-Teller effect interacts with the physical angular momentum. Through this interaction, as demonstrated in two hypothetical experiments, a circularly polarized light pulse induces the rotation of the entire molecule, as presented in Sec. I C.

Conversely, in the covalent case discussed in Sec. II, the Jahn-Teller effect arises from the atomic displacements affecting the electron covalent bonding, Sec. II B, and does not directly involve the molecule's rotation angle, as shown in Sec. II C. However, the chiral normal modes now possess a physical angular momentum, even though, lacking an electric dipole, they cannot directly couple to an electromagnetic field. Nonetheless, through the virtual photoexcitation of an optically active particle-hole pair, that subsequently de-excite via Jahn-Teller coupling, the electromagnetic field can couple to the chiral modes, making them detectable in the infrared absorption spectrum, as discussed in sections II D and II E. A similar phenomenon occurs, for instance, in doped C_{60} and explains the optical absorption at the frequency of the T_{1u} modes [16]. In this context, we also propose in Sec. II E a hypothetical experiment where a circularly polarized light in resonance with the chiral normal modes can induce rotational motion in the molecule.

I. D_3 SYMMETRIC IONIC MOLECULE

The first toy model we study refers to an ionic molecule that exhibits D_3 planar symmetry, depicted schematically in Fig. 1. Even though we do not intend to faithfully describe any real molecule, we could nonetheless imagine that the physics we are going to describe might be pertinent, e.g., to metal trifluoride MF_3 (M=Al, Sc, Y), which is indeed a planar ionic molecule.

We adopt a reference frame in which the position of the

* Contact author: gstaffie@sissa.it

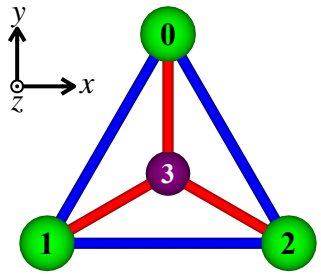

FIG. 1: Toy planar molecule with D_3 symmetry. The bonds represent springs with spring constants K, the blue bonds, and γK, the red ones.

$\boldsymbol{D_3}$	E	C_3	C_2'
A_1	1	1	1
A_2	1	1	-1
E	2	-1	0

	A_1	A_2	E
A_1	A_1	A_2	E
A_2	A_2	A_1	E
E	E	E	$A_1 \oplus [A_2] \oplus E$

TABLE I: Character table, left, and product table, right, of the wallpaper group D_3. The antisymmetric product of two identical irreducible representations is indicated by square brackets.

central ion, numbered as 3 and with purple color in Fig. 1, is fixed, but the molecule can freely rotate around that position, with rotation angle ϕ. The three external ions, numbered from 0 to 2 and drawn in green, have equal mass M and are symmetrically located around the central one with an equilibrium distance that we take as our unit of length. From now on, we disregard the out-of-plane ionic motion. Consequently, the point group is the two-dimensional D_3 that includes, besides the identity E, the threefold rotation C_3 around atom 3 and the twofold rotation C_2' around the y-axis and its equivalent axes by C_3 symmetry. The character and product tables of the irreducible representations (irreps) are shown in Table I. Following the Appendix, we parametrize the positions of the green atoms, $n = 0, 1, 2$, as

$$\mathbf{r}_n = \mathbf{R}_n + \mathbf{x}_n = \big(1 + \alpha_n\big)\,\mathbf{R}_n + \beta_n\,\boldsymbol{z} \wedge \mathbf{R}_n\,, \tag{1}$$

with $\boldsymbol{z}$ the unit vector perpendicular to the plane of the molecule,

$$\mathbf{R}_n = C_{n2\pi/3}\big(\mathbf{R}_0\big)\,, \quad \mathbf{R}_0 = (0, 1)\,, \tag{2}$$

the equilibrium positions, with C_θ representing the rotation by an angle θ around the central atom, and $\mathbf{x}_n$ the n-th ion displacement. We further write, see (A.3),

$$\begin{pmatrix} \alpha_n \\ \beta_n \end{pmatrix} = \frac{1}{\sqrt{3}} \sum_{\ell=-1}^{1} \mathrm{e}^{ik_\ell n}\,\mathbf{q}_\ell\,, \tag{3}$$

where $k_\ell = 2\pi\ell/3$, $\ell = -1, 0, +1$. As discussed in the Appendix, to avoid double counting the variable ϕ that describes the molecular rotation with respect to a fixed reference frame, the vector $\mathbf{q}_\ell$ for $\ell = 0$ has only one component that differs from zero, i.e.,

$$\mathbf{q}_0 = \begin{pmatrix} q_{A_1} \\ 0 \end{pmatrix}\,,$$

and describes the A_1 breathing mode. On the contrary, $\mathbf{q}_\ell = \mathbf{q}_{-\ell}^*$ for $\ell = \pm 1$ have both components finite and transform as the two-dimensional irrep E. The atomic Hamiltonian has the general form, see (A.9),

$$\begin{aligned} H_{\rm at} = \frac{\big(p_\phi - \mathrm{L}_{\rm vib}\big)^2}{2I} + \frac{p_{A_1}^2}{2M} \\ + \frac{1}{2M} \sum_{\ell \neq 0} \mathbf{p}_\ell \cdot \mathbf{p}_{-\ell} + V\big(\{\mathbf{r}_n\}\big)\,, \end{aligned} \tag{4}$$

where p_ϕ is the momentum conjugate to ϕ and equals the total angular momentum L, while p_{A_1} is conjugate to q_{A_1} and, for $\ell = \pm 1$, $\mathbf{p}_{-\ell}$ conjugate to $\mathbf{q}_\ell$. The operator

$$\mathrm{L}_{\rm vib} = \sum_{\ell = \pm 1} \mathbf{q}_\ell \wedge \mathbf{p}_{-\ell} \cdot \boldsymbol{z}\,, \tag{5}$$

is the contribution of the vibrational modes to the angular momentum, sometimes called the *spin* of the phonons, and $I = M\,\big(\sqrt{3} + q_{A_1}\big)^2$ the moment of inertia.
The eigenstates of (4) can be classified in terms of the irreps A_1 and E in Table I. In particular, the operator (5) transforms as A_2, which implies that it couples eigenstates with symmetry E, see the product rules in Table I.

A. Inter atomic potential in the harmonic approximation

To simplify the analysis, we adopt the harmonic approximation for the interatomic potential, which is quite valid in AlF_3 [17, 18] as well as in ScF_3 and Y_3 [19]. Specifically, we assume that the blue and red bonds in Fig. 1 have, respectively, spring constants K and γK, with $\gamma \gg 1$ [17], consistently with the ionic nature of the red bonds. Therefore, using the parametrization (1), $V\big(\{\mathbf{r}_n\}\big)$ in the harmonic approximation is simply

$$\begin{aligned} V\big(\{\mathbf{r}_n\}\big) = \frac{\gamma K}{2} \sum_{n=0}^{2} \alpha_n^2 \\ + \frac{K}{8} \sum_{n=0}^{2} \Big(\sqrt{3}\,\big(\alpha_{n+1} + \alpha_n\big) + \big(\beta_{n+1} - \beta_n\big)\Big)^2\,. \end{aligned} \tag{6}$$

The normal modes are obtained by diagonalizing the dynamical matrix. This is readily accomplished using (3), leading to the eigenvalue equations for the dynamical matrix

$$\lambda_\ell^2\,\mathbf{u}_\ell = \begin{pmatrix} \varepsilon_\ell + A_\ell & iB_\ell \\ -iB_\ell & \varepsilon_\ell - A_\ell \end{pmatrix}\,\mathbf{u}_\ell\,, \tag{7}$$

where λ_ℓ^2 are the eigenvalues in units of K, $B_\ell = -B_{-\ell} = \sin k_\ell \sqrt{3}/2$ and

$$\varepsilon_\ell = \frac{\gamma + 2 + \cos k_\ell}{2} \,, \quad A_\ell = \frac{\gamma + 1 + 2\cos k_\ell}{2} \,.$$

The eigenvalues are therefore

$$\lambda_{1\ell}^2 = \epsilon_\ell - \sqrt{A_\ell^2 + B_\ell^2} \,, \quad \lambda_{2\ell}^2 = \epsilon_\ell + \sqrt{A_\ell^2 + B_\ell^2} \,, \quad (8)$$

and the corresponding eigenvectors read

$$\mathbf{u}_{1\ell} = \begin{pmatrix} -i\sin\theta_\ell \\ \cos\theta_\ell \end{pmatrix} \,, \quad \mathbf{u}_{2\ell} = \begin{pmatrix} \cos\theta_\ell \\ -i\sin\theta_\ell \end{pmatrix} \,,$$

where

$$\theta_\ell = -\theta_{-\ell} = \frac{1}{2}\,\tan^{-1}\frac{B_\ell}{A_\ell} \,.$$

For $\ell = 0$, where $\theta_0 = 0$, only the mode 2 with eigenvalue $\lambda_{20}^2 = \lambda_{A_1}^2 = 3 + \gamma$ must be considered, and corresponds to the A_1 breathing mode with normal mode coordinate q_{A_1}. The modes with $\ell = +1$ are characterized by

$$\begin{aligned} &\theta_1 = \theta = \frac{1}{2}\,\tan^{-1}\frac{3}{2\gamma} \xrightarrow[\gamma\gg 1]{} \frac{3}{4\gamma} \ll 1 \,, \\ &\lambda_{1+1}^2 = \lambda_1^2 \xrightarrow[\gamma\gg 1]{} \frac{5}{4} \,, \qquad \lambda_{2+1}^2 = \lambda_2^2 \xrightarrow[\gamma\gg 1]{} \gamma + \frac{1}{4} \,, \end{aligned} \quad (9)$$

and are degenerate with the $\ell = -1$ ones that have $\theta_{-1} = -\theta$. For $\ell = \pm 1$ we introduce the normal mode coordinates, $q_{1\ell}$ and $q_{2\ell}$, and momenta, $p_{1\ell}$ and $p_{2\ell}$. Correspondingly, the coordinate, $\mathbf{q}_\ell$, and momentum, $\mathbf{p}_\ell$, operators in (4) and (5) become

$$\mathbf{q}_\ell = q_{1\ell}\,\mathbf{u}_{1\ell} + q_{2\ell}\,\mathbf{u}_{2\ell} \,, \quad \mathbf{p}_\ell = p_{1\ell}\,\mathbf{u}_{1\ell} + p_{2\ell}\,\mathbf{u}_{2\ell} \,.$$

We find more convenient to introduce real normal mode coordinates through the canonical transformation

$$q_{a\pm 1} = \frac{1}{\sqrt{2}}\left(q_{ax} \pm i\, q_{ay}\right) \,, \quad a = 1, 2 \,,$$

and similarly for the conjugate momenta. In terms of the new conjugate operators, Eq. (5) reads

$$\begin{aligned} \mathrm{L}_{\rm vib} = &-\sin 2\theta \left(\mathbf{q}_1 \wedge \mathbf{p}_1 - \mathbf{q}_2 \wedge \mathbf{p}_2\right) \\ &- \cos 2\theta \left(\mathbf{q}_1 \wedge \mathbf{p}_2 + \mathbf{q}_2 \wedge \mathbf{p}_1\right) , \end{aligned} \quad (10)$$

where $\mathbf{q}_a$, $a = 1, 2$, is the vector with components q_{ax} and q_{ay}. The Hamiltonian (4) in the harmonic approximation has the simple expression

$$\begin{aligned} H_{\rm at} = &\frac{1}{2I}\left(p_\phi - \mathrm{L}_{\rm vib}\right)^2 + \frac{1}{2M}\sum_j p_j^2 \\ &+ \frac{K}{2}\sum_j \lambda_j^2\, q_j^2 \,, \end{aligned} \quad (11)$$

where $j = A_1, 1x, 1y, 2x, 2y$ and, we recall,

$$I = M\left(\sqrt{3} + q_{A_1}\right)^2 . \quad (12)$$

The normal modes are shown in Fig. 2 for large γ.

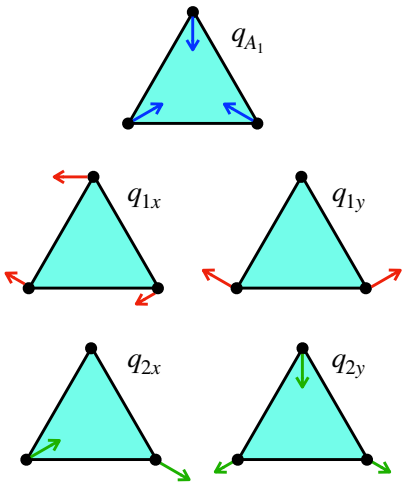

FIG. 2: Sketch of the normal modes of the molecule in Fig. 1 in the limit $\gamma \gg 1$.

B. Jahn-Teller coupling

The electron molecular orbitals (MOs) can also be classified based on the irreducible representations in Table I, or, more precisely, the irreps of the point group D_{3h}. Let us here consider a MO that transforms like the two-dimensional irrep E, $E' \sim (x, y)$ in D_{3h}, and explore the Jahn-Teller coupling with the ionic displacements. For simplicity, we restrict our analysis to the linear order in the ionic displacement. Later, we will discuss the effects of the second-order term. The electrons on the E-type MO feel a crystal field potential

$$\begin{aligned} U &= \sum_{n=0}^{2} U\big(|\mathbf{r} - \mathbf{r}_n|\big) = \sum_{n=0}^{2} U\big(\,|\mathbf{r} - \mathbf{R}_n|\,\big) \\ &\quad + \sum_{n=0}^{2}\Big\{U\big(\,|\mathbf{r} - \mathbf{R}_n - \mathbf{x}_n|\,\big) - U\big(\,|\mathbf{r} - \mathbf{R}_n|\,\big)\Big\} \\ &= U_0 + U_{\rm JT} \,, \end{aligned} \quad (13)$$

where $\mathbf{r}$ is the electron coordinate, U_0 the potential due to the atoms in their equilibrium positions $\mathbf{R}_n$, while $U_{\rm JT}$ is the correction caused by the atomic displacements, which starts linear in $\mathbf{x}_n$. It follows that U_0 is invariant under D_3, and therefore cannot split the MO. On the contrary, $U_{\rm JT}$ can lift the MO twofold degeneracy by the Jahn-Teller effect. To find an explicit expression of $U_{\rm JT}$, we assume the MO localized on the central atom, 3 in Fig. 1, so that $|r| \ll |\mathbf{R}_n|$, and expand $U_{\rm JT}$ up to second order in $\mathbf{r}$ and at first order in the atomic displacements. The first order correction in $\mathbf{r}$ gives no contribution since the two orbitals have the same odd parity. The calculation of the second order correction in $\mathbf{r} = r\,(\cos\phi_e, \sin\phi_e)$ is simple but tedious, therefore we present here just the

final result

$$U_{\rm JT} = \frac{3r^2}{4}\Big\{ g_1\Big(\cos 2\big(\phi-\phi_e\big)\, q_{1y} + \sin 2\big(\phi-\phi_e\big)\, q_{1x}\Big) + g_2\Big(\cos 2\big(\phi-\phi_e\big)\, q_{2y} + \sin 2\big(\phi-\phi_e\big)\, q_{2x}\Big)\Big\}, \tag{14}$$

where

$$g_1 = U_1\,\sin\theta + U_2\,\cos\theta\,, \quad g_2 = U_1\,\cos\theta - U_2\,\sin\theta\,,$$

and

$$U_1 = -\frac{1}{2}\big(\partial U - \partial^2 U + \partial^3 U\big)\,, \quad U_2 = -\big(\partial U - \partial^2 U\big)\,,$$

with $\partial^n U$ the n-th derivative of $U\big(|\mathbf{r}-\mathbf{R}_n|\big)$ calculated at $\mathbf{r}=\mathbf{0}$, thus at $|\mathbf{r}-\mathbf{R}_n| = |\mathbf{R}_n| = 1$. The potential (14) projected onto the MO subspace, with orbitals $p_x(\mathbf{r}) \sim \psi(r)\,\cos\phi_e$ and $p_y(\mathbf{r}) \sim \psi(r)\,\sin\phi_e$, realizes a standard $e\times E$ Jahn-Teller effect with a peculiar property. Indeed, the full Hamiltonian, including $U_{\rm JT}$ in (14), preserves the operator

$$\mathrm{L}_{\rm TOT} = \mathrm{L} + \mathrm{L}_e = -i\left(\frac{\partial}{\partial\phi} + \frac{\partial}{\partial\phi_e}\right), \tag{15}$$

which we can legitimately regard as the total, electrons plus ions, angular momentum. A posteriori, this result is in no way surprising, since the total Hamiltonian must be invariant under global planar rotations. However, this property is not often emphasized and, as we are going to show, leads to interesting phenomena.

C. Hypothetical experiments

Here and in Section II E, we explore how a light pulse circularly polarized in the plane of the molecule can induce molecular rotations. We will consider this possibility in a highly idealized setup: an isolated molecule struck by the laser pulse. A more realistic scenario could involve molecules in the gas phase within a cylindrical vessel that can rotate around its axis, and a light pulse with circular polarization perpendicular to that axis. In this case, we must also account for additional complications, such as intermolecular interactions, the interaction between the molecules and the vessel wall, and the thermally randomized orientation of the molecule planes relative to the light polarization. Although such an experiment can be envisioned, we cannot predict whether the desired resulting rotation of the vessel would be measurable. Therefore, we restrict our analysis to the somewhat unrealistic setup of an isolated molecule.

In the specific case of the molecule in Fig. 1, since $\gamma \gg 1$, the lowest energy normal mode is the mode $\mathbf{q}_1$ with symmetry E and frequency $\omega_1 \equiv \omega_0 \simeq \sqrt{5K/4M}$. It describes displacements perpendicular to the equilibrium positions $\mathbf{R}_n$, the q_{1x} and q_{1y} modes of Fig. 2. In what follows, we neglect all other higher energy modes, so that the moment of inertia (12) becomes constant, $I \simeq 3M$. Since $\gamma \gg 1$ also implies $\theta \simeq 0$, see (9), the contribution of the normal mode 1 to the angular momentum in (10) can be neglected. We observe that the off-diagonal term in (10), which remains finite for $\theta \to 0$, can still provide mode 1 with an angular momentum at second order perturbation theory. However, such term for $\gamma \gg 1$ is of the same order as the diagonal one $\propto \sin 2\theta$, and thus equally negligible. We mention that there are instead circumstances in which off-diagonal terms in $\mathrm{L}_{\rm vib}$ may play the major role [11].

Focusing, as before, on an E-type MO, the total Hamiltonian, sum of (11) and (14), can therefore be written as

$$H \simeq H_{\rm at} + U_{\rm JT} = \frac{p_\phi^2}{2I} + \frac{\omega_0}{2}\left(\mathbf{p}^2+\mathbf{q}^2\right) - g\sum_\sigma \Big\{ q_x\,\Psi_\sigma^\dagger\left(\cos 2\phi\,\tau_3 + \sin 2\phi\,\tau_1\right)\Psi_\sigma + q_y\,\Psi_\sigma^\dagger\left(\sin 2\phi\,\tau_3 - \cos 2\phi\,\tau_1\right)\Psi_\sigma\Big\}, \tag{16}$$

where $\mathbf{q}$ and $\mathbf{p}$ are dimensionless conjugate variables with components q_a and p_a, $a = x, y$, defined as

$$q_a = \sqrt{M\omega_0}\; q_{1a}\,, \quad p_a = \sqrt{\frac{1}{M\omega_0}}\; p_{1a}\,.$$

The spinor Ψ_σ in (16) is defined as

$$\Psi_\sigma = \begin{pmatrix} c_{x\sigma} \\ c_{y\sigma} \end{pmatrix},$$

with components the annihilation operators of the MO orbitals p_x and p_y with spin σ, and τ_α, $\alpha = 1,2,3$, the Pauli matrices that act in the orbital space. In this representation, the electron angular momentum reads

$$\mathrm{L}_e = \sum_\sigma \Psi_\sigma^\dagger\,\tau_2\,\Psi_\sigma\,,$$

and $\mathrm{L}_{\rm TOT} = p_\phi + \mathrm{L}_e$ is conserved. We apply a $\pi/2$ rotation around τ_1, so that $\tau_2 \to \tau_3$, $\tau_3 \to -\tau_2$ and thus

$$\Psi_\sigma \to \begin{pmatrix} c_{+1\sigma} \\ c_{-1\sigma} \end{pmatrix}, \quad \mathrm{L}_e \to \sum_\sigma \Psi_\sigma^\dagger\,\tau_3\,\Psi_\sigma\,.$$

Moreover, we define

$$q_x = -\frac{i}{2}\big(a_+ - a_+^\dagger - a_- + a_-^\dagger\big)\,,$$
$$q_y = -\frac{1}{2}\big(a_+ + a_+^\dagger + a_- + a_-^\dagger\big)\,,$$

and accordingly p_x and p_y, where $a_\pm$ and $a_\pm^\dagger$ are bosonic annihilation and creation operators, respectively, so that

$$H = \frac{p_\phi^2}{2I} + \omega_0 \left(n_+ + n_- + 1\right) - g \sum_\sigma \Big\{ \left(a_+ + a_-^\dagger\right) \Psi_\sigma^\dagger \, \mathrm{e}^{-i2\phi} \, \tau_+ \, \Psi_\sigma + \left(a_+^\dagger + a_-\right) \Psi_\sigma^\dagger \, \mathrm{e}^{i2\phi} \, \tau_- \, \Psi_\sigma^\dagger \Big\} , \tag{17}$$

with $n_\pm = a_\pm^\dagger \, a_\pm$, which further emphasizes the existence of another conserved quantity of H, specifically,

$$\mathrm{J} = n_+ - n_- + \frac{1}{2} \, \mathrm{L}_e \, , \tag{18}$$

which plays the role of a pseudo angular momentum.
We note that J assumes integer values when the number of electrons on the MO is even, and half-integer values when the number of electrons is odd, which is the case we are interested in. The latter property is unique to a linear Jahn-Teller coupling. In the presence of a second-order term in the atomic displacement, and as its coupling strength increases, the pseudo angular momentum J at odd occupation of the MO quite abruptly crossovers from being quantized in half-integer values to being quantized in integer values [20], the 1/2 in (18) simply replaced by 1. Nevertheless, a pseudo angular momentum can still be defined and differs from the physical one for the simple fact that the mode 1 carries no angular momentum. Therefore, despite our focus on the linear order term, which notably simplifies the calculations, we anticipate no qualitative changes in the presence of a second-order correction.

Although our primary objective is to demonstrate how chiral normal modes can be excited by light and subsequently induce molecular rotation, we begin by presenting a different hypothetical experimental scenario. In this scenario, light is employed to generate an electronic excitation, and we show how, through the Jahn-Teller coupling, this excitation is transformed into a molecule's rotation.
We assume that the above E-type MO is empty in the ground state, which has vanishing total angular momentum. However, we can envision a scenario where, at $t = 0$, the molecule is in an excited state characterized by one electron in that molecular orbital with $\mathrm{L}_e = +1$, yet no excited bosons. This possibility could arise, for instance, if an ultrafast circularly-polarized light pulse were to transfer one electron from an occupied MO of symmetry A_1 to the unoccupied MO of symmetry E. It follows that the initial values of total and pseudo angular momenta are $\mathrm{L_{TOT}} = 1$ and $\mathrm{J} = 1/2$, and they remain so under the unitary evolution with Hamiltonian (17). Along this evolution, L_e jumps between +1 and -1 and, correspondingly, $n_+ - n_-$ between 0 and +1, so as to maintain $\mathrm{J} = 1/2$ constant. Therefore, the contribution of the rigid body rotation to the angular momentum

$$p_\phi = I \, \dot{\phi} = \mathrm{L_{TOT}} - \mathrm{L}_e = 1 - \mathrm{L}_e \, ,$$

jumps between 0 and 2, namely the molecule acquires an angular acceleration after the purely electronic excitation.
To simulate the actual dynamics, we construct the Lanczos chain where the first site $\ell = 1$ is the initial state, i.e., $|1\rangle = c_{+1}^\dagger \, |0\rangle$, with $|0\rangle$ the electron and boson vacuum. In this way we can formally rewrite (17) as

$$H = \sum_{\ell \geq 1} t_\ell \left(|\ell + 1\rangle \langle \ell| + |\ell\rangle \langle \ell + 1| \right) + \sum_{\ell \geq 1} \epsilon_\ell \, |\ell\rangle \langle \ell| \, , \tag{19}$$

where the parameters can be easily derived and read

$$t_\ell = \begin{cases} -g \sqrt{\ell/2} \, , & \ell = \text{even} \, , \\ -g \sqrt{(\ell+1)/2} \, , & \ell = \text{odd} \, , \end{cases}$$

$$\epsilon_\ell = \omega_0 \, \ell + \begin{cases} 2/I \, , & \ell = \text{even} \, , \\ 0 \, , & \ell = \text{odd} \, , \end{cases}$$

while the sites of the chain correspond to the wavefunctions

$$|\ell = 2n+1\rangle = \frac{1}{\sqrt{2\pi}} \, \frac{a_+^{\dagger \, n} \, a_-^{\dagger \, n}}{n!} \, c_{+1}^\dagger \, |0\rangle \, ,$$

$$|\ell = 2n+2\rangle = \frac{\mathrm{e}^{2i\phi}}{\sqrt{2\pi}} \, \frac{a_+^{\dagger \, n+1} \, a_-^{\dagger \, n}}{\sqrt{n! \, (n+1)!}} \, c_{-1}^\dagger \, |0\rangle \, ,$$

with $n \geq 0$. In other words, on the odd sites $\mathrm{L}_e = +1$ and thus $p_\phi = 0$, while on the even ones $\mathrm{L}_e = -1$ and $p_\phi = 2$. In this representation, the wavefunction at time t can be written as

$$|\psi(t)\rangle = \sum_{\ell \geq 1} \psi_\ell(t) \, |\ell\rangle \, ,$$

where the components $\psi_\ell(t)$ satisfy the equation of motion

$$i \, \dot{\psi}_\ell(t) = \epsilon_\ell \, \psi_\ell(t) + t_{\ell-1} \, \psi_{\ell-1}(t) + t_\ell \, \psi_{\ell+1}(t) \, ,$$

with boundary conditions $\psi_\ell(0) = \delta_{\ell,1}$ and $\psi_{\ell=0}(t) = 0$. Therefore, the unitary evolution of the initial state transforms into the propagation of a particle on the Lanczos chain that starts on the first site at $t = 0$. It follows that

$$p_\phi(t) = \langle \psi(t)| \, p_\phi \, |\psi(t)\rangle = 2 \sum_{n \geq 1} \left|\psi_{2n}(t)\right|^2 .$$

In Fig. 3 we plot the angular velocity $\dot{\phi}(t) = p_\phi(t)/I$. We observe that, since the dynamics does not account for the anticipated de-excitation of the electron, $\dot{\phi}(t)$ continues to oscillate between zero and a finite positive value. However, if we considered the finite lifetime of

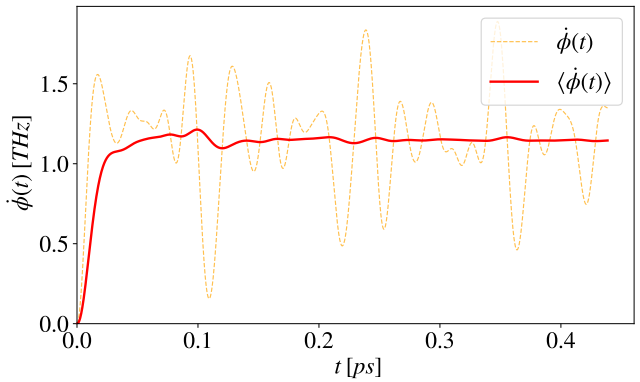

FIG. 3: Time evolution of the angular velocity $\dot\phi(t) = p_\phi(t)/I$, and its time-average $\langle\dot\phi(t)\rangle$, obtained by integrating the Lanczos chain defined in (19). The undamped oscillations over time result from the exchange of angular momentum between the molecule and the electron in the singly occupied E-type molecular orbital during the unitary evolution. The chosen parameters correspond to those of AlF_3, with $\omega_0 = \nu_4 \simeq 240\ \mathrm{cm}^{-1}$ [17], a moment of inertia $I \simeq 36$ in units of $\hbar^2/\omega_0$. The Jahn-Teller coupling g obtained through (14) is $1.8\,\omega_0$.

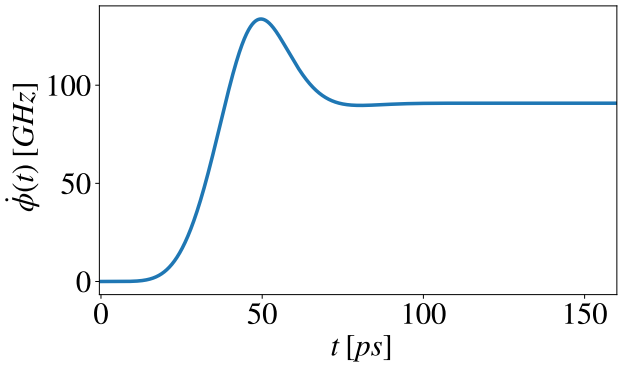

FIG. 4: Time evolution of $\dot\phi(t)$ induced by a circularly polarized electric field pulse in resonance with the chiral mode 1 of Fig. 3. For times longer than the pulse duration, i.e., $t \gtrsim 100$ ps, $\dot\phi(t)$ becomes constant. The frequency and moment of inertia are the same as in Fig. 3. We take $\tau = 33$ ps, the electric field maximum amplitude $E_0 = 800$ kV/cm, and estimate $d_* = 0.1\ e$Å.

the electronic excitation, and that were substantially longer than the time scale $1/\omega_0$, around 0.1 ps for AlF_3, we would expect a behavior similar to the time average of $\dot\phi(t)$ shown in Fig. 3, which converges to a finite value. We emphasize that this qualitative behavior holds irrespective of the harmonic approximation and the linear Jahn-Teller coupling. Indeed, the absorption of the circularly polarized light implies that a finite angular momentum is initially supplied to the electrons. This angular momentum is subsequently transferred to the molecular vibrations in the form of a pseudo angular angular momentum, see (18) with the 1/2 eventually replaced by 1 if the second order Jahn-Teller coupling is dominant. However, since the molecular vibration does not carry any physical angular momentum, this process must inevitably be accompanied by a transfer of physical angular momentum to the molecule, which begins rotating.

Now, we delve into another hypothetical experiment that is more pertinent to our objectives. We observe that, because the molecule is ionic, the mode 1 with $\ell = \pm 1$ carries a dipole moment $\boldsymbol{d} = d_*\,(q_x, q_y)$, see Fig. 2, with d_* the dipole strength, and therefore couples directly to an electric field. Let us therefore consider a circularly polarized electric field in the reference frame of the molecule,

$$\boldsymbol{E}(t) = E(t)\,\big(\cos(\omega t - \phi), \sin(\omega t - \phi)\big)\,,$$

with $E(t)$ an envelope function finite in a time interval $t \in [0, \tau]$. With all MOs either fully occupied or empty, the Hamiltonian (17) becomes

$$\begin{aligned} H(t) = {} & \frac{p_\phi^2}{2I} + \omega_0\,\Big(n_+ + n_- + 1\Big) \\ & - i\,\frac{d_*\,E(t)}{2}\,\Big\{ \mathrm{e}^{i(\omega t - \phi)}\,\big(a_+^\dagger + a_-\big) \\ & \qquad - \mathrm{e}^{-i(\omega t - \phi)}\,\big(a_+ + a_-^\dagger\big)\Big\}\,, \end{aligned} \tag{20}$$

and admits as conserved quantity the pseudo angular momentum

$$\mathrm{J} = p_\phi + n_+ - n_-\,. \tag{21}$$

We apply the time independent unitary transformation

$$U = \mathrm{e}^{-i\phi(n_+ - n_-)}\,, \tag{22}$$

after which $H(t) \to H'(t) = U^\dagger\,H(t)\,U$, where

$$\begin{aligned} H'(t) = {} & \frac{1}{2I}\,\big(p_\phi - n_+ + n_-\big)^2 \\ & + \omega_0\,\Big(n_+ + n_- + 1\Big) \\ & - i\,\frac{d_*\,E(t)}{2}\,\Big\{ \mathrm{e}^{i\omega t}\,\big(a_+^\dagger + a_-\big) \\ & \qquad - \mathrm{e}^{-i\omega t}\,\big(a_+ + a_-^\dagger\big)\Big\}\,. \end{aligned} \tag{23}$$

We remark that p_ϕ is in fact the conserved pseudo angular momentum (21) after the unitary transformation. At $t < 0$, before the field is turned on, we assume that the molecule has no excited boson and has $p_\phi = 0$, which remains zero along the subsequent time evolution. If

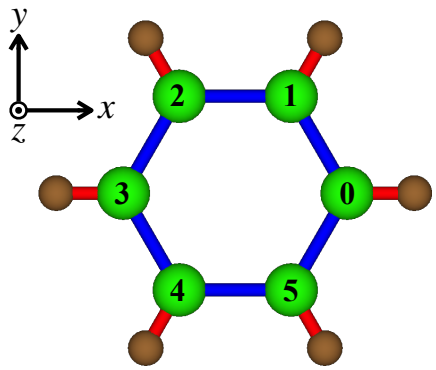

FIG. 5: Toy planar molecule with D_6 symmetry.

$|\psi(t)\rangle$ is the time-dependent wavefunction, solution of the Schrœdinger equation $i\,|\dot\psi(t)\rangle = H'(t)\,|\psi(t)\rangle$, then

$$\begin{aligned}\dot\phi(t) &= -i\,\langle\psi(t)|\left[\phi, H'(t)\right]|\psi(t)\rangle \\ &= -\frac{1}{I}\,\langle\psi(t)|\,n_+ - n_-\,|\psi(t)\rangle\,,\end{aligned}$$

which we show in Fig. 4. We take an envelope function

$$E(t) = E_0\left(\frac{t}{\tau}\right)^2 \exp\left\{1-\left(\frac{t}{\tau}\right)^2\right\},$$

which describes an electric pulse that reaches a peak amplitude E_0 at $t=\tau$, and then decays exponentially fast. When the field is on, $0 < t \gtrsim \tau$, $\dot\phi(t)$ increases until a maximum and then it converges to a lower but finite value for $t \gg \tau$, when the field is turned off and the Hamiltonian becomes again independent of ϕ. Therefore, the electric field pulse is able to induce a permanent rotation of the entire molecule. We remark that the inclusion of high-energy modes and eventually anharmonic terms will cause $\dot\phi(t)$ to oscillate even for $t \gg \tau$, potentially leading to dephasing due to interference between different oscillation frequencies. Nevertheless, we anticipate that the long-time average of $\dot\phi(t)$ will remain finite as long as dissipation from the environment can be neglected.

II. D_6 SYMMETRIC COVALENT MOLECULE

The next example we consider is the planar molecule in Fig. 5 that has D_6 symmetry. This molecule evidently reminds benzene, C_6H_6, with C atoms in green and H ones in brown. In what follows, we do use such analogy without pretending to give an accurate description of real benzene.

As before we use a reference frame in which the centre of the molecule is fixed, while we define as ϕ the angle that describes the rotation of the molecule around the z axis, see Fig. 5. Furthermore, we project out the high-energy C-H breathing mode and neglect out-of-plane atomic displacements. Therefore, the point group of the molecule can be approximated with the two dimensional D_6 that contains the sixfold, C_6, threefold, C_3, and twofold, C_2, rotations around z, as well as twofold rotations around x, C_2', and y, C_2''. Real benzene, due to its out-of-plane degrees of freedom, instead exhibits D_{6h} point group symmetry, complemented by the x-y mirror plane. The character and product tables of the irreducible representations (irreps) of D_6 are shown in Table II. Following the Appendix, the positions of the green atoms, $n = 0,\dots,5$, in Fig. 5 is parametrized through

$\boldsymbol{D_6}$	E	C_6	C_3	C_2	C_2'	C_2''
A_1	1	1	1	1	1	1
A_2	1	1	1	1	−1	−1
B_1	1	−1	1	−1	1	−1
B_2	1	−1	1	−1	−1	1
E_1	2	1	−1	−2	0	0
E_2	2	1	−1	2	0	0

	A_1	A_2	B_1	B_2	E_1	E_2
A_1	A_1	A_2	B_1	B_2	E_1	E_2
A_2	A_2	A_1	B_2	B_1	E_1	E_2
B_1	B_1	B_2	A_1	A_2	E_2	E_1
B_2	B_2	B_1	A_2	A_1	E_2	E_1
E_1	E_1	E_1	E_2	E_2	$A_1 \oplus [A_2] \oplus E_2$	$B_1 \otimes B_2 \otimes E_1$
E_2	E_2	E_2	E_1	E_1	$B_1 \otimes B_2 \otimes E_1$	$A_1 \oplus [A_2] \oplus E_2$

TABLE II: Character table, top, and product table, bottom, of the wallpaper group D_6. The antisymmetric product of two identical irreducible representations is indicated by square brackets.

$$\mathbf{r}_n = \mathbf{R}_n + \mathbf{x}_n = \big(1+\alpha_n\big)\,\mathbf{R}_n + \beta_n\,\boldsymbol{z}\wedge\mathbf{R}_n\,,$$

where $\mathbf{x}_n$ is the displacement with respect to the equilibrium positions

$$\mathbf{R}_n = C_{\phi+(n-1)\pi/3}\big(\mathbf{R}_0\big)\,,\quad \mathbf{R}_0 = (1,0)\,.$$

We make the change of variables (A.3)

$$\begin{pmatrix}\alpha_n\\ \beta_n\end{pmatrix} = \frac{1}{\sqrt{N}}\sum_\ell \mathrm{e}^{ik_\ell n}\,\mathbf{q}_\ell\,, \tag{24}$$

now with

$$k_\ell = \frac{2\pi}{6}\,\ell\,,\quad \ell = -2,\dots,3\,.$$

As discussed earlier, $\mathbf{q}_0$ has only the first component finite, which corresponds to the A_1 breathing mode to which we associate the coordinate q_{A_1}. The displacement $\mathbf{q}_{+1} = \mathbf{q}_{-1}^*$ transforms like the irrep E_1, while $\mathbf{q}_{+2} = \mathbf{q}_{-2}^*$ like the irrep E_2. Finally, the first component q_{B_1} of $\mathbf{q}_3$

transforms like B_1, while the second component q_{B_2} like B_2, thus the notation. The atomic Hamiltonian (A.9) reads in this case

$$H_{\rm at} = \frac{\left(p_\phi - {\rm L}_{\rm vib}\right)^2}{2I} + \frac{p_{A_1}^2}{2M} + \frac{p_{B_1}^2}{2M} + \frac{p_{B_2}^2}{2M} + \frac{1}{2M}\sum_{\ell\pm1,\pm2} \mathbf{p}_\ell\cdot\mathbf{p}_{-\ell} + V\big(\{\mathbf{r}_n\}\big)\,, \tag{25}$$

where the moment of inertia is

$$I = M\left(\sqrt{6} + q_{A_1}\right)^2, \tag{26}$$

and the displacement contribution to the angular momentum has the expression

$${\rm L}_{\rm vib} = q_{B_1}\,p_{B_2} - q_{B_2}\,p_{B_1} + \sum_{\ell\pm1,\pm2} \mathbf{q}_\ell\wedge\mathbf{p}_{-\ell}\cdot\boldsymbol{z}\,. \tag{27}$$

We note that the combinations that appear in (27) are consistent with ${\rm L}_{\rm vib}$ transforming like A_2 and the product Table II.

A. Inter atomic potential in the harmonic approximation

As in the previous case, we discuss the normal modes assuming the harmonic approximation for the inter atomic potential $V\big(\{\mathbf{r}_n\}\big)$. We mention that anharmonic effects in benzene are not significant except for the C-H stretching modes [21],which we do not take into account anyway.

We therefore consider the blue bonds in Fig. 5, which we approximate as springs with stiffness K and equilibrium length that we take as unit of length. The inter atomic potential thus reads

$$V\big(\{\mathbf{r}_n\}\big) = \frac{K}{8}\sum_n \Big[\big(\alpha_{n+1}+\alpha_n\big) + \sqrt{3}\,\big(\beta_{n+1}-\beta_n\big)\Big]^2. \tag{28}$$

In addition to (28), we include a further harmonic potential δV with spring constant $\gamma\,K$, $\gamma\ll1$ [22], which is minimum when the angle between three successive carbon atoms is 120° and refers to the fact that the energy is lower when the carbon atoms are in the sp^2 configuration. Specifically,

$$\delta V\big(\{\mathbf{r}_n\}\big) = \frac{\gamma K}{8}\sum_n \Big(\alpha_{n+1} - \sqrt{3}\,\beta_{n+1} + \alpha_{n-1} + \sqrt{3}\,\beta_{n-1} - 2\alpha_n\Big)^2. \tag{29}$$

The normal modes of the dynamical matrix solve an eigenvalue equation similar to (7)

$$\lambda_\ell^2\,\mathbf{u}_\ell = \begin{pmatrix} \varepsilon_\ell + A_\ell & iB_\ell \\ -iB_\ell & \varepsilon_\ell - A_\ell\end{pmatrix}\mathbf{u}_\ell\,, \tag{30}$$

where λ_ℓ^2 are the eigenvalues in units of K, and

$$\begin{aligned}
\varepsilon_\ell &= \frac{1}{2}\big(2 - \cos k_\ell + 3\gamma - 2\gamma\cos k_\ell - \gamma\cos 2k_\ell\big)\,,\\
A_\ell &= \frac{1}{2}\big(-1 + 2\cos k_\ell - 2\gamma\cos k_\ell + 2\gamma\cos 2k_\ell\big)\,,\\
B_\ell &= \frac{\sqrt{3}}{2}\big(\sin k_\ell + 2\gamma\sin k_\ell - \gamma\sin 2k_\ell\big)\,.
\end{aligned} \tag{31}$$

Upon defining

$$\theta_\ell = -\theta_{-\ell} = \frac{1}{2}\,\tan^{-1}\frac{B_\ell}{A_\ell}\,,$$

the eigenvalues of (30) read

$$\lambda_{1\ell}^2 = \varepsilon_\ell - \sqrt{A_\ell^2 + B_\ell^2}\,,\quad \lambda_{2\ell}^2 = \varepsilon_\ell + \sqrt{A_\ell^2 + B_\ell^2}\,,$$

with the corresponding eigenmodes

$$\mathbf{u}_{1\ell} = \begin{pmatrix} i\sin\theta_\ell \\ \cos\theta_\ell\end{pmatrix},\quad \mathbf{u}_{2\ell} = \begin{pmatrix} \cos\theta_\ell \\ i\sin\theta_\ell\end{pmatrix}.$$

Since $\gamma\ll1$, $\lambda_{1\ell}^2 \ll \lambda_{2\ell}^2$ for any ℓ. For $\ell=0$, we must consider only the mode 2 that corresponds to q_{A_1} and has eigenvalue $\lambda_{20}^2 = \lambda_{A_1}^2$. Conversely, for $\ell=3$ mode 1 corresponds to q_{B_2} and mode 2 to q_{B_1}, with eigenvalues $\lambda_{13}^2 = \lambda_{B_2}^2$ and $\lambda_{23}^2 = \lambda_{B_1}^2$, respectively. Finally, for $\ell = \pm1,\pm2$ we introduce the normal mode coordinates $q_{1\ell}$ and $q_{2\ell}$, as well as the corresponding conjugate momenta $p_{1\ell}$ and $p_{2\ell}$, so that, as before,

$$\mathbf{q}_\ell = q_{1\ell}\,\mathbf{u}_{1\ell} + q_{2\ell}\,\mathbf{u}_{2\ell}\,,$$

and similarly for $\mathbf{p}_\ell$. By symmetry, the modes at ℓ and $-\ell$ are degenerate. The atomic Hamiltonian (25) within the harmonic approximation thus reads

$$\begin{aligned}
H_{\rm at} = {}& \frac{1}{2I}\Big(p_\phi - {\rm L}_{\rm vib}\Big)^2 + \frac{p_{A_1}^2}{2M} + \frac{K\lambda_{A_1}^2}{2}\,q_{A_1}^2\\
&+ \frac{p_{B_1}^2}{2M} + \frac{K\lambda_{B_1}^2}{2}\,q_{B_1}^2\\
&+ \frac{p_{B_2}^2}{2M} + \frac{K\lambda_{B_2}^2}{2}\,q_{B_2}^2\\
&+ \sum_{a=1,2}\sum_{\ell=\pm1,\pm2}\left(\frac{1}{M}\,p_{a\ell}\,p_{a\ell}^\dagger + K\,\lambda_{a\ell}^2\,q_{a\ell}\,q_{a\ell}^\dagger\right).
\end{aligned} \tag{32}$$

where the contribution of the normal modes to the total angular momentum is

$$\begin{aligned}
{\rm L}_{\rm vib} = {}& \Big(q_{B_1}\,p_{B_2} - q_{B_2}\,p_{B_1}\Big)\\
&+ \sum_{\ell=1}^{2}\Big\{i\,\sin 2\theta_\ell\,\big(q_{1\ell}\,p_{1-\ell} - q_{1-\ell}\,p_{1\ell}\\
&\qquad - q_{2\ell}\,p_{2-\ell} + q_{2-\ell}\,p_{2\ell}\big)\\
&\quad - \cos 2\theta_\ell\,\Big(q_{1\ell}\,p_{2-\ell} + q_{1-\ell}\,p_{2\ell}\\
&\qquad - q_{2\ell}\,p_{1-\ell} - q_{2-\ell}\,p_{1\ell}\Big)\Big\}.
\end{aligned} \tag{33}$$

We observe that the two combinations

$$\begin{aligned} L_1^+ &= \cos\Big(\frac{\pi}{4} - \theta_1\Big)\; q_{1+1} \\ &\quad - i\,\sin\Big(\frac{\pi}{4} - \theta_1\Big)\; q_{2+1}\,, \\ L_2^+ &= i\,\sin\Big(\frac{\pi}{4} - \theta_1\Big)\; q_{1-1} \\ &\quad + \cos\Big(\frac{\pi}{4} - \theta_1\Big)\; q_{2-1}\,, \end{aligned} \tag{34}$$

act like rising operators for $\mathrm{L_{vib}}$ in (33), thus the hermitian conjugates of (34) as lowering ones. One can readily obtain analogous operators for $\ell = \pm 2$ and for the B modes.

B. Electron Hamiltonian

We assume that each green atom in Fig. 5 hosts a p_z orbital occupied by one electron. At fixed atomic positions, the electron Hamiltonian is simply a tight-binding on a hexagon with nearest, t_1, next nearest, t_2, and next to next nearest, t_3, hopping amplitudes, with $t_1 > t_2 > t_3 > 0$. Therefore, the single-particle eigenstates have eigenvalues

$$\epsilon_\ell = -2\sum_{j=1}^{3} t_j\,\cos k_\ell j\,, \quad \ell = -2,\dots,3\,.$$

We assume that the hopping amplitudes are such that $\epsilon_3 > \epsilon_{\pm 2} > \epsilon_{\pm 1} > \epsilon_0$. The state with $\ell = 0$ transforms like the A_1 irrep of D_6, that with $\ell = 3$ like the B_1 irrep, while the two doublets with $\ell = \pm 1$ and $\ell = \pm 2$, respectively, like the two dimensional irreps $E_1 \sim Y_{1,\pm 1}$ and $E_2 \sim Y_{2,\pm 2}$.

1. *Electronic moment of inertia and magnetic orbital moment*

We suppose that the molecule rotates with constant angular velocity ω, thus the green atom equilibrium positions are time-dependent $\mathbf{R}_n \to \mathbf{R}_n(t)$, $n = 0,\dots,5$. The single-electron Hamiltonian in first quantization is therefore

$$H(t) = \frac{\mathbf{p}^2}{2m} + \sum_{n=0}^{5} U\big(\mathbf{r} - \mathbf{R}_n(t)\big)\,,$$

with m the electron mass, and the Schrödinger equation reads, accordingly,

$$i\,\frac{d\psi(\mathbf{r},t)}{dt} = H(t)\,\psi(\mathbf{r},t)\,.$$

We use the standard trick and make a change of variable using the reference frame in which the atoms are at rest, thus

$$\mathbf{r} \to \mathbf{r}(t) = \cos\omega t\;\mathbf{r} + \sin\omega t\;\mathbf{r}\times\boldsymbol{z}\,,$$

and assume $\psi(\mathbf{r},t) \to \phi(\mathbf{r}(t),t)$ so that

$$\begin{aligned} i\,\frac{d\phi(\mathbf{r}(r),t)}{dt} &= i\,\frac{\partial\phi(\mathbf{r}(r),t)}{\partial t} \\ &\quad - \omega\,\mathbf{r}(t)\times\boldsymbol{z}\cdot\mathbf{p}\,\phi(\mathbf{r}(r),t)\,. \end{aligned}$$

In this reference frame $U(\mathbf{r} - \mathbf{R}_n(t)) \to U(\mathbf{r}(t) - \mathbf{R}_n)$. Since only the explicit time-derivative appears, we can replace $\mathbf{r}(t) \to \mathbf{r}$ and get the effective Schrödinger equation

$$\begin{aligned} i\,\frac{\partial\phi(\mathbf{r},t)}{\partial t} &= \Big\{H + \omega\,\mathbf{r}\times\boldsymbol{z}\cdot\mathbf{p}\Big\}\,\phi(\mathbf{r},t) \\ &= H(\omega)\,\phi(\mathbf{r},t)\,, \end{aligned} \tag{35}$$

now with time-independent Hamiltonian. The solution is simply obtained: if $\phi_a(\mathbf{r})$ is any eigenstate of $H(\omega)$ with eigenvalue $\epsilon_a(\omega)$, then $\phi_a(\mathbf{r},t) = \mathrm{e}^{-i\epsilon_a(\omega)t}\;\phi_a(\mathbf{r})$. As a matter of fact, $H(\omega)$ looks like the Hamiltonian in presence of a fictitious magnetic field generated by a vector potential

$$\boldsymbol{A}(\mathbf{r}) = \frac{\omega mc}{e}\,\mathbf{r}\times\boldsymbol{z} = \frac{\omega mc}{e}\,\big(y,-x\big)\,.$$

In reality,

$$\begin{aligned} &\frac{\mathbf{p}^2}{2m} + \frac{e}{mc}\,\boldsymbol{A}(\mathbf{r})\cdot\mathbf{p} \\ &= \frac{1}{2m}\left(\mathbf{p} + \frac{e}{c}\,\boldsymbol{A}(\mathbf{r})\right)^2 - \frac{m\omega^2}{2}\,r^2 \\ &\simeq \frac{1}{2m}\left(\mathbf{p} + \frac{e}{c}\,\boldsymbol{A}(\mathbf{r})\right)^2 - \frac{m\omega^2}{2}\,, \end{aligned}$$

since the electron coordinates are localized around the atomic positions, all of which are at unit distance from the origin.

Assuming the Peierls approximation and, for simplicity, just the nearest neighbor hopping t_1, the fictitious magnetic field adds a phase

$$\Phi = \frac{\sqrt{3}}{2}\,\omega\,m\,,$$

so that the eigenstates of $H(\omega)$ are the same $\psi_\ell(\mathbf{r})$ of the tight-binding Hamiltonian, but now have eigenvalues

$$\begin{aligned} \varepsilon_\ell(\omega) &= -2\,t_1\,\cos\big(k_\ell + \Phi\big) - \frac{m\omega^2}{2} \\ &= \epsilon_\ell(\omega) - \frac{m\omega^2}{2}\,. \end{aligned}$$

I note that, since $\boldsymbol{A}(\mathbf{r}) \propto \omega$,

$$\frac{\partial H(\omega)}{\partial\omega} = \frac{e}{\omega mc}\,\boldsymbol{A}(\mathbf{r})\cdot\mathbf{p}\,,$$

so that

$$\begin{aligned} &\int d\mathbf{r}\,\psi_\ell(\mathbf{r})^*\left(\frac{e}{mc}\,\boldsymbol{A}(\mathbf{r})\cdot\mathbf{p}\right)\psi_\ell(\mathbf{r}) \\ &= \omega\int d\mathbf{r}\,\psi_\ell(\mathbf{r})^*\,\frac{\partial H(\omega)}{\partial\omega}\,\psi_\ell(\mathbf{r}) \\ &= \omega\,\frac{\partial\varepsilon_\ell(\omega)}{\partial\omega} = \Phi\,\frac{\partial\epsilon_\ell(\omega)}{\partial\Phi} - m\omega^2\,, \end{aligned}$$

because also $\Phi \propto \omega$. The actual value $E_\ell(\omega)$ of the energy of the state $\psi_\ell(r,t) = \mathrm{e}^{-i\epsilon_\ell(\omega)t}\ \phi_\ell(\mathbf{r}(t))$ expanded at second order in ω is

$$\begin{aligned} E_\ell(\omega) &= i \int d\mathbf{r}\, \psi_\ell(r,t)^* \ \frac{d\psi_\ell(r,t)}{dt} \\ &= \int d\mathbf{r}\, \psi_\ell(\mathbf{r})^* \left(\varepsilon_\ell(\omega) - \frac{e}{mc}\, \boldsymbol{A}(\mathbf{r}) \cdot \mathbf{p} \right) \psi_\ell(\mathbf{r}) \\ &= \epsilon_\ell(\omega) - \frac{m\omega^2}{2} - \Phi\ \frac{\partial \epsilon_\ell(\omega)}{\partial \Phi} + m\omega^2 \\ &\simeq \epsilon_\ell + \frac{m\omega^2}{2} + \frac{3}{8}\,\omega^2\, m^2\, \epsilon_\ell\,, \end{aligned} \tag{36}$$

which implies that the moment of inertia of an electron in the wavefunction $\psi_\ell(\mathbf{r})$ is

$$I_\ell = m\, \left(1 + \frac{3}{4}\, m\, \epsilon_\ell \right)\,.$$

We note that $\sum_\sigma \sum_\ell I_\ell = 12m$, so that, if all levels are occupied, the electronic contribution to the moment of inertia is the expected one. On the contrary, in the case with 6 electrons that we consider, the moment of inertia

$$I_e = \sum_\sigma \sum_{\ell=-1}^{1} I_\ell = 6m - 3t_1\, m^2\,,$$

is reduced with respect to the bare value $6m$, a kind of diamagnetic response to angular rotations.
We can repeat the calculations above assuming that the molecule is pierced by a real magnetic flux and readily find that each electron state carries a magnetic orbital moment L_ℓ given by

$$\mathrm{L}_\ell = \mu_B\, \sqrt{3}\, m\, t_1\, \sin \frac{\pi \ell}{3}\ . \tag{37}$$

C. Coupling to the normal modes

We assume that the hopping between sites n and $n+m$ is a decaying function of their distance $|\mathbf{r}_{n+m} - \mathbf{r}_n|$. It follows that, for small displacements $\mathbf{x}_n$ and $\mathbf{x}_{n+m}$, $m = 1,2,3$,

$$\begin{aligned} t_m\big(|\mathbf{r}_{n+m} - \mathbf{r}_n|\big) &\simeq t_m \Big\{ 1 - g_m c_m \left(\alpha_{n+m} + \alpha_n \right) \\ &\qquad - g_m s_m \left(\beta_{n+1} - \beta_n \right) \Big\} \\ &\equiv t_m - \delta t_m\,, \end{aligned} \tag{38}$$

where g_m is the coupling constant and

$$c_m = \cos \frac{\pi(3-m)}{6}\ , \quad s_m = \sin \frac{\pi(3-m)}{6}\ .$$

It follows that the coupling between the electrons and the normal modes is

$$\begin{aligned} V_{\text{el-vib}} &= \sum_{m=1}^{3} \delta t_m \sum_{n\sigma} \left(c^\dagger_{n+m\sigma}\, c_{n\sigma} + c^\dagger_{n\sigma}\, c_{n+m\sigma} \right) \\ &= \frac{1}{\sqrt{6}} \sum_m g_m\, t_m \sum_\sigma \sum_{\ell_1 \ell_2} c^\dagger_{\ell_1 \sigma}\, c_{\ell_2 \sigma} \\ &\qquad \left(\mathrm{e}^{-imk_{\ell_1}} + \mathrm{e}^{imk_{\ell_2}} \right) \\ &\qquad \Big\{ c_m\, a_{\ell_1 - \ell_2} \left(\mathrm{e}^{imk_{\ell_1 - \ell_2}} + 1 \right) \\ &\qquad + s_m\, b_{\ell_1 - \ell_2} \left(\mathrm{e}^{imk_{\ell_1 - \ell_2}} - 1 \right) \Big\}\,, \end{aligned} \tag{39}$$

where $\ell_2 + \ell_3$ or $\ell - \ell_2$ are defined modulo 6 with integers between -2 and 3. It is worth emphasizing that the momentum conservation in (39) simply reflects the invariance of the Hamiltonian with respect to the D_3 point group.
We note that the coupling to the normal modes vanishes identically whenever $\mathrm{e}^{-imk_{\ell_1}} + \mathrm{e}^{imk_{\ell_2}} = 0$, namely, when

$$m\left(\ell_1 + \ell_2\right) = 3(1+2n)\,, \quad m = 1,2,3\,.$$

In particular, the normal mode assisted tunneling between the electronic states with $\ell = \pm 1$ and those with $\ell = \pm 2$ only occurs via the next-nearest neighbor hopping t_2, an observation that we use later.

D. Coupling to a circularly polarized electromagnetic field

We assume that a circularly polarized electromagnetic field (EMF) is applied to the molecule, with

$$\boldsymbol{E}(t) = E\, \big(\cos \omega t, \sin \omega t \big)\,,$$

and thus vector potential

$$\boldsymbol{A}(t) = \frac{cE}{\omega}\, \big(-\sin \omega t, \cos \omega t \big)\,.$$

In the reference frame of the molecule, which is rotated by ϕ,

$$\boldsymbol{A}(t,\phi) = \frac{cE}{\omega}\, \Big(\sin(\phi - \omega t), \cos(\phi - \omega t) \Big)\,.$$

The bonds that connect atom n with $n+m$ are the vectors $\mathbf{R}_{n,m}$, $m = 1,2,3$, given by

$$\begin{aligned} \boldsymbol{R}_{n,m} &= \mathbf{R}_{n+m} - \mathbf{R}_n \\ &= \left(\cos \frac{(2n+3+m)\pi}{6}\,, \sin \frac{(2n+3+m)\pi}{6} \right)\,. \end{aligned} \tag{40}$$

It follows that the Peierls phase acquired by the hopping term $c^\dagger_{n+m\sigma}\, c_{n\sigma}$ is

$$\begin{aligned}\phi_{n,m} &= \frac{e}{c}\, \boldsymbol{A}(t,\phi)\cdot \boldsymbol{R}_{n,m} \\ &= \frac{eE}{\omega}\, \sin\Big((2n+3+m)\pi/6 - \phi - \omega t\Big) \\ &= -i\,\frac{eE}{2\omega}\,\Big(\mathrm{e}^{i\frac{\pi}{6}(3+m)}\, \mathrm{e}^{i(\phi-\omega t)}\, \mathrm{e}^{in\pi/3} - c.c.\Big) \\ &\equiv Q_m\, \mathrm{e}^{i(\phi-\omega t)}\, \mathrm{e}^{in\pi/3} + c.c.\,,\end{aligned}$$

and behaves like the sum of a Bloch wave with momentum k_1 and one with k_{-1}. The first order correction in the EMF to the hopping Hamiltonian thus reads

$$\begin{aligned}\delta T = -i\,\mathrm{e}^{i(\phi-\omega t)} \sum_m Q_m\, t_m \sum_\sigma \sum_{\ell_1\ell_2\ell_3} c^\dagger_{\ell_1\sigma}\, c_{\ell_2\sigma} \\ \Big(\mathrm{e}^{-ik_{\ell_1} m} - \mathrm{e}^{ik_{\ell_2} m}\Big)\Big\{\delta_{\ell_1,\ell_2+1} \\ - \frac{g_m}{\sqrt{6}}\, c_m\, a_{\ell_1-\ell_2-1}\Big(\mathrm{e}^{ik_{\ell_1-\ell_2-1}m} + 1\Big) \\ - \frac{g_m}{\sqrt{6}}\, s_m\, b_{\ell_1-\ell_2-1}\Big(\mathrm{e}^{ik_{\ell_1-\ell_2-1}m} - 1\Big)\Big\} \\ + H.c.\,.\end{aligned} \tag{41}$$

As expected, the circularly polarized light can induce on its own electronic excitations with $\Delta\ell = \pm 1$, or with different $\Delta\ell$ in cooperation with the molecular vibrations. We also note from (41) that, if the electronic configuration is prepared in a finite current state, i.e., with

$$J = \sum_m t_m \sum_{\ell\sigma} \sin k_\ell m\, \langle\, c^\dagger_{\ell\sigma}\, c_{\ell\sigma}\,\rangle \neq 0\,,$$

then the light couples directly to the normal modes with $\ell = \pm 1$, despite the molecule is non-polar and thus the vibrations are not charged. This is not the sole such possibility, as we are going to show.

E. Hypothetical experiment

We assume that the molecule contains six electrons and therefore the electronic ground state has occupied $\ell = 0, \pm 1$ levels. If the EMF frequency ω and the energy of the normal mode 1 with $\ell = \pm 1$ are close to each other and much smaller than $\epsilon_{\ell=\pm 2} - \epsilon_{\ell=\pm 1} \equiv \Delta$, a coupling between the electromagnetic field and the normal mode is generated by second order perturbation theory [16]. For simplicity, we only consider in (41) the field induced excitations from the occupied $\ell = \pm 1$ to the empty $\ell = \pm 2$ without involvement of the molecular vibrations and limited to the dominant nearest neighbor hopping. In this case,

$$\begin{aligned}\delta T &\simeq -\frac{eEt_1}{\omega} \sum_\sigma \Big\{\mathrm{e}^{i(\phi-\omega t)}\; c^\dagger_{2\sigma}\, c_{1\sigma} \\ &\qquad + \mathrm{e}^{-i(\phi-\omega t)}\; c^\dagger_{-2\sigma}\, c_{-1\sigma}\Big\} + H.c. \\ &\equiv \delta T^+ + \delta T^-\,.\end{aligned} \tag{42}$$

Concerning the coupling between electrons and normal modes, we just focus on the mode with $\ell = \pm 1$ that is also able to transfer one electron from $\ell = \pm 1$ to $\ell = \pm 2$. As previously discussed, the coupling term (39) vanishes for nearest neighbor hopping. We therefore consider the next-nearest neighbor one, in which case (39) reads, through (34),

$$\begin{aligned}V_{\text{el-vib}} \simeq -i\, g_2\, t_2 \sum_\sigma \Big\{c^\dagger_{2\sigma}\, c_{1\sigma}\; L_1^+ + c^\dagger_{-2\sigma}\, c_{-1\sigma}\; L_1^-\Big\} \\ + H.c. \equiv V^+_{\text{el-vib}} + V^-_{\text{el-vib}}\,.\end{aligned} \tag{43}$$

It follows that, if $|n\rangle$ are the electronic eigenstates with eigenvalues E_n, with $|0\rangle$ the ground state, then, by second order perturbation theory,

$$\begin{aligned}V_{\text{EMF-vib}} &= \sum_{n>0}\Bigg\{\frac{\langle 0|\,\delta T^-\,|n\rangle\,\langle n|\,V^+_{\text{el-vib}}\,|0\rangle}{E_n - E_0} \\ &\qquad + \frac{\langle 0|\,V^-_{\text{el-vib}}\,|n\rangle\,\langle n|\,\delta T^+\,|0\rangle}{E_n - E_0}\Bigg\} \\ &= 2i\;\frac{eE}{\omega}\;\frac{g_2\, t_1\, t_2}{\Delta}\Big\{\mathrm{e}^{-i(\phi-\omega t)}\; L_1^+ + H.c.\Big\}\,.\end{aligned} \tag{44}$$

In other words, the virtual excitation of a particle-hole pair with $\Delta\ell = \pm 1$ mediates a coupling between the EMF and the chargeless normal modes, rendering the latter observable in the infrared spectrum [16]. We also note that (44) has a conserved pseudo angular momentum

$$\mathrm{J} = p_\phi + \mathrm{L}_{\text{vib}} = \mathrm{L} + \mathrm{L}_{\text{vib}}\,. \tag{45}$$

Therefore, the EMF is able not only to excite the normal modes with $\ell = \pm 1$ but also to change the total angular momentum L of the molecule.
Since $\gamma \ll 1$, the angle $\theta_1 \simeq \pi/4$, thus $L_1^+ \simeq q_{1+1}$ and

$$\begin{aligned}V_{\text{EMF-vib}} \simeq 2i\;\frac{eE}{\omega}\;\frac{g_2\, t_1\, t_2}{\Delta} \\ \Big\{\mathrm{e}^{-i(\phi-\omega t)}\; q_{1+1} - \mathrm{e}^{i(\phi-\omega t)}\; q_{1-1}\Big\}\,.\end{aligned} \tag{46}$$

We define dimensionless normal mode coordinates through

$$q_{1\pm1} \to \sqrt{K_1}\; q_{1\pm1}\,, \quad p_{1\pm1} \to \frac{1}{\sqrt{K_1}}\; p_{1\pm1}\,,$$

with $K_1 = 1/M\omega_0$ and $\omega_0 = \lambda_{1\pm1}\sqrt{K/M}$ the normal mode energy. The $a = 1$ and $\ell = \pm 1$ contribution to L_{vib} is therefore

$$\mathrm{L}_{\text{vib}} = i\,\Big(q_{1+1}\, p_{1-1} - q_{1-1}\, p_{1+1}\Big)\,. \tag{47}$$

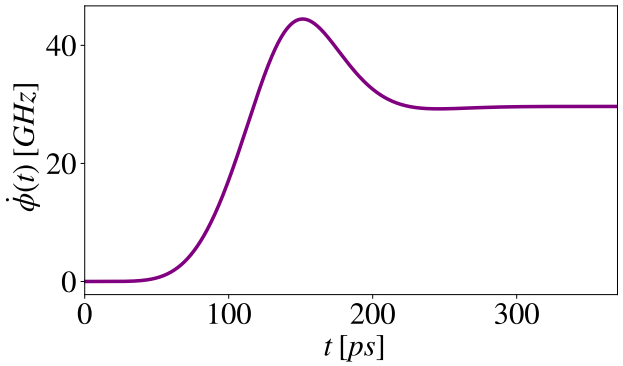

FIG. 6: Time evolution of $\dot{\phi}(t)$ in the benzene-like molecule induced by a circularly polarized electric field pulse in resonance with the E_{1u} C-H bending mode. The qualitative behavior is the same as the one shown for the D_3 molecule in Fig. 4. The C-C bond length is taken as 1.413 Å [22], while the frequency of the E_{1u} phonon as $\omega_0 = 1048\,\mathrm{cm}^{-1}$ [23]. The dipole associated to the phonon is $d_* = 9.5 \cdot 10^{-4}\, e$Å [24] and the moment of inertia in units of $\hbar^2/\omega_0$ is $I \simeq 123$. We take $\tau = 101$ ps and the electric field maximum amplitude $E_0 = 10$ MV/cm.

We further define

$$q_{1\,+1} = \frac{1}{\sqrt{2}}\left(a_- + a_+^\dagger\right), \quad p_{1\,-1} = \frac{i}{\sqrt{2}}\left(a_-^\dagger - a_+\right),$$

so that

$$\mathrm{L}_{\mathrm{vib}} = a_+^\dagger\, a_+ - a_-^\dagger\, a_- = n_+ - n_- \,. \tag{48}$$

The simplified Hamiltonian $H(t)$ in presence of the EMF reads therefore

$$\begin{aligned} H(t) = \frac{1}{2I}\Big(p_\phi - n_+ + n_-\Big)^2 \\ + \omega_0\Big(n_+ + n_- + 1\Big) \\ + i\,E(t)\,\gamma\Big\{\mathrm{e}^{-i(\phi-\omega t)}\,\left(a_- + a_+^\dagger\right) \\ - \mathrm{e}^{i(\phi-\omega t)}\,\left(a_+ + a_-^\dagger\right)\Big\}, \end{aligned} \tag{49}$$

where γ is a constant and $E(t)$ an envelope function that grows from zero at $t > 0$ and remains finite for a finite time interval τ. We observe that (49) resembles (20), except that the normal modes now carry an angular momentum that enters explicitly in (49). That would make the molecule rotate even if ϕ did not appeared explicitly. We plot the time evolution of $\dot{\phi}$ in Fig. 6. Unsurprisingly, the dynamical behavior remains qualitatively the same as that in Fig. 4 of Sec. I C.

III. CONCLUSIONS

We have shown how circularly polarized light can induce angular rotation of molecules that possess coupled doubly degenerate electronic orbitals and (chiral) normal modes that realize an $e \times E$ Jahn-Teller effect. This coupling is invariant under $U(1)$ rotations with generator a pseudo angular momentum distinct from the physical one. In particular, we have considered two exemplary cases: a D_3 symmetric ionic molecule and a D_6 symmetric covalent one, inspired, respectively, by metal trifluorides and by benzene. The Jahn-Teller effect originates from the dependence of the crystal field on the ion displacements within the ionic molecule, and, in the covalent case, of the electron covalent bonding on the atomic displacements, thereby providing a comprehensive representation of all possible physical realizations.
Although our results are specific to two molecular toy models, certain aspects might be relevant also to bulk systems. For instance, the interaction between circularly polarized light and the chiral normal modes of bulk crystalline samples can be direct in ionic materials or mediated by virtual particle-hole excitations in covalent systems. In either case, this coupling depends on the relative angle ϕ between the sample reference frame and the laboratory frame. Consequently, the light can drive the sample into rotation, inducing a finite angular velocity $\dot{\phi}$. Furthermore, if the chiral modes independently contribute to the physical angular momentum, as observed in the benzene molecule, their coherent excitation, regardless of its realization [10–13], might yield comparable effects to circularly polarized light.

ACKNOWLEDGMENTS

The authors are very grateful to Antimo Marrazzo for stimulating discussions that inspired the work.

Appendix: Derivation of the Hamiltonian

In this Appendix, we derive the expression for the atomic Hamiltonian of a planar molecule with a regular N-sided polygon shape and equivalent atoms of mass M at its vertices. As in the main text, we disregard out-of-plane displacements. Consequently, the point group of the molecule is the two-dimensional D_N. We also neglect the motion of the center of mass, which coincides with the center of the polygon, but we account for the molecule's rotations around this point. Our objective is to separate the global molecule rotation from all internal degrees of freedom, which is straightforward in this regular geometry.
The atoms at the vertices are at position $\mathbf{r}_n$, $n = 0, \ldots, N-1$, which we parametrize as

$$\mathbf{r}_n = \mathbf{R}_n + \mathbf{x}_n = \big(1 + \alpha_n\big)\,\mathbf{R}_n + \beta_n\,\boldsymbol{z} \wedge \mathbf{R}_n \,, \tag{A.1}$$

where $\mathbf{R}_n$ are the equilibrium positions, $\boldsymbol{z}$ the unit vector perpendicular to the molecule plane, and $\mathbf{x}_n$ the displacements. By symmetry,

$$\mathbf{R}_n = C_{n2\pi/N}\big(\mathbf{R}_0\big)\,, \quad n = 0, \dots, N-1\,,$$

where C_θ is a rotation by an angle θ around the centre of the molecule. Hereafter, we set $|\mathbf{R}_0| = 1$ our unit of length.

We denote by ϕ the dynamical rotation angle of the molecule with respect to a fixed reference frame. Consistently, we must exclude the displacements that also correspond to a global molecule rotation. With the parametrization (A.1), this amounts to impose that

$$\sum_n \beta_n = \sum_n \mathbf{x}_n \cdot \boldsymbol{z} \wedge \mathbf{R}_n = \sum_n \mathbf{r}_n \cdot \boldsymbol{z} \wedge \mathbf{R}_n \equiv 0\,, \quad \text{(A.2)}$$

which implies that also the time derivatives vanish. To enforce (A.2), we make the unitary transformation

$$\begin{aligned} \begin{pmatrix} \alpha_n \\ \beta_n \end{pmatrix} &= \frac{1}{\sqrt{N}} \sum_\ell \mathrm{e}^{ik_\ell n} \begin{pmatrix} a_\ell \\ b_\ell \end{pmatrix} \\ &= \frac{1}{\sqrt{N}} \sum_\ell \mathrm{e}^{ik_\ell n}\, \mathbf{q}_\ell\,, \end{aligned} \quad \text{(A.3)}$$

where $k_\ell = 2\pi\ell/N$, $\ell = -\lceil N/2\rceil + 1, \dots, \lfloor N/2\rfloor$ are the wave vectors corresponding to an N-site chain with periodic boundary conditions, and $\mathbf{q}_\ell = \mathbf{q}^*_{-\ell}$. In this representation, the constraint (A.2) simply implies that $b_0 \equiv 0$. Therefore, $\mathbf{q}_0$ has only one component a_0. Another advantage of (A.3) is that $\mathbf{q}_\ell$ transform automatically as the irreducible representations of the point group. For instance, a_0 represents the A_1 breathing mode, and so we define $a_0 \coloneqq q_{A_1}$.

With respect to the fixed reference frame, the atomic positions read

$$\mathbf{r}_n(\phi) = C_\phi\big(\mathbf{r}_n\big) = \cos\phi\, \mathbf{r}_n + \sin\phi\, \boldsymbol{z} \wedge \mathbf{r}_n\,,$$

thus

$$\dot{\mathbf{r}}_n(\phi) = C_\phi\big(\dot{\mathbf{r}}_n + \dot\phi\, \boldsymbol{z} \wedge \mathbf{r}_n\big) = C_\phi\big(\dot{\mathbf{x}}_n + \dot\phi\, \boldsymbol{z} \wedge \mathbf{r}_n\big)\,. \quad \text{(A.4)}$$

Therefore, taking the constraint (A.2) into account and using (A.3), the angular momentum L has the expression

$$\begin{aligned} \mathrm{L} &= M \sum_n \mathbf{r}_n(\phi) \wedge \dot{\mathbf{r}}_n(\phi) \cdot \boldsymbol{z} \\ &= M \sum_n \mathbf{r}_n \wedge \big(\dot{\mathbf{r}}_n + \dot\phi\, \boldsymbol{z} \wedge \mathbf{r}_n\big) \cdot \boldsymbol{z} \\ &= \dot\phi\, M \sum_n \mathrm{r}_n^2 + M \sum_n \mathbf{x}_n \wedge \dot{\mathbf{x}}_n \cdot \boldsymbol{z} \\ &\coloneqq \dot\phi\, I_0 + M \sum_{\ell\neq 0} \mathbf{q}_\ell \wedge \dot{\mathbf{q}}_{-\ell} \cdot \boldsymbol{z} \coloneqq \dot\phi\, I_0 + J\,, \end{aligned} \quad \text{(A.5)}$$

where we remark that $\ell = N/2 \equiv -N/2$ for even N, and we can write

$$\begin{aligned} J &= M \sum_{\ell\neq 0} \mathbf{q}_\ell \wedge \dot{\mathbf{q}}_{-\ell} \cdot \boldsymbol{z} = M \sum_{\ell\neq 0} \dot{\mathbf{q}}_\ell \cdot \boldsymbol{z} \wedge \mathbf{q}_{-\ell}\,, \\ I_0 &= M\left(\sqrt{N} + q_{A_1}\right)^2 + M \sum_{\ell\neq 0} \mathbf{q}_\ell \cdot \mathbf{q}_{-\ell} \\ &\coloneqq I + M \sum_{\ell\neq 0} \mathbf{q}_\ell \cdot \mathbf{q}_{-\ell} \coloneqq I + \delta I\,, \end{aligned}$$

with I the total moment of inertia. Similarly, the kinetic energy reads

$$\begin{aligned} T &= \frac{M}{2} \sum_n \dot{\mathbf{r}}_n(\phi) \cdot \dot{\mathbf{r}}_n(\phi) \\ &= \frac{M}{2} \sum_n \big(\dot{\mathbf{x}}_n + \dot\phi\, \boldsymbol{z} \wedge \mathbf{r}_n\big) \cdot \big(\dot{\mathbf{x}}_n + \dot\phi\, \boldsymbol{z} \wedge \mathbf{r}_n\big) \\ &= \frac{I_0}{2}\, \dot\phi^2 + J\, \dot\phi + \frac{M}{2}\, \dot q_{A_1}^2 + \frac{M}{2} \sum_{\ell\neq 0} \dot{\mathbf{q}}_\ell \cdot \dot{\mathbf{q}}_{-\ell}\,. \end{aligned} \quad \text{(A.6)}$$

By definition, the variables p_ϕ, p_{A_1} and $\mathbf{p}_{-\ell}$ conjugate to ϕ, q_{A_1} and $\mathbf{q}_\ell$, respectively, are obtained through

$$\begin{aligned} p_\phi &= \frac{\partial T}{\partial \dot\phi} = \dot\phi\, I_0 + J \equiv \mathrm{L}\,, \\ p_{A_1} &= \frac{\partial T}{\partial \dot q_{A_1}} = M\, \dot q_{A_1}\,, \\ \mathbf{p}_{-\ell} &= \frac{\partial T}{\partial \dot{\mathbf{q}}_\ell} = M\, \dot{\mathbf{q}}_{-\ell} + \dot\phi\, \frac{\partial J}{\partial \dot{\mathbf{q}}_\ell}\,. \end{aligned} \quad \text{(A.7)}$$

Conversely,

$$\begin{aligned} \dot\phi &= \frac{p_\phi - J}{I_0}\,, \qquad \dot q_{A_1} = \frac{p_{A_1}}{M}\,, \\ \dot{\mathbf{q}}_\ell &= \frac{1}{M}\left(\mathbf{p}_\ell - \dot\phi\, \frac{\partial J}{\partial \dot{\mathbf{q}}_{-\ell}}\right). \end{aligned}$$

It follows that

$$\begin{aligned} J &= \sum_{\ell\neq 0} \dot{\mathbf{q}}_\ell \cdot \frac{\partial J}{\partial \dot{\mathbf{q}}_\ell} \\ &= \sum_{\ell\neq 0} \mathbf{q}_\ell \wedge \mathbf{p}_{-\ell} \cdot \boldsymbol{z} - \frac{\dot\phi}{M} \sum_{\ell\neq 0} \frac{\partial J}{\partial \dot{\mathbf{q}}_\ell} \cdot \frac{\partial J}{\partial \dot{\mathbf{q}}_{-\ell}} \\ &\coloneqq \mathrm{L}_{\mathrm{vib}} - \dot\phi\, M \sum_{\ell\neq 0} \mathbf{q}_\ell \cdot \mathbf{q}_{-\ell} = \mathrm{L}_{\mathrm{vib}} - \dot\phi\, \delta I \\ &= \mathrm{L}_{\mathrm{vib}} - \frac{\delta I}{I_0}\, \big(p_\phi - J\big)\,, \end{aligned}$$

namely,

$$J = \frac{I_0\, \mathrm{L}_{\mathrm{vib}} - \delta I\, p_\phi}{I}\,,$$

and thus

$$\dot\phi = \frac{p_\phi - \mathrm{L}_{\mathrm{vib}}}{I}\,. \quad \text{(A.8)}$$

Therefore, if $V\big(\{\mathbf{r}_n\}\big)$ is the inter atomic potential, minimum at $\mathbf{r}_n = \mathbf{R}_n$ and independent of ϕ, the atomic Hamiltonian is defined through

$$H_{\rm at} = p_\phi\,\dot{\phi} + p_{A_1}\,\dot{q}_{A_1} + \sum_{\ell\neq 0} \mathbf{p}_{-\ell}\cdot\dot{\mathbf{q}}_\ell - T + V\big(\{\mathbf{r}_n\}\big)\,,$$

which, using the above results, can be readily expressed in terms of conjugate variables as

$$\begin{aligned} H_{\rm at} = {} & \frac{\big(p_\phi - \mathrm{L}_{\rm vib}\big)^2}{2I} + \frac{p_{A_1}^2}{2M} \\ & + \frac{1}{2M}\sum_{\ell\neq 0}\mathbf{p}_\ell\cdot\mathbf{p}_{-\ell} + V\big(\{\mathbf{r}_n\}\big)\,. \end{aligned} \tag{A.9}$$

We emphasize that (A.9) is valid regardless of the form of the interatomic potential and can be straightforwardly quantized.

[1] A. Einstein and W. de Haas, Experimenteller Nachweis der Ampereschen Molekularströme, Verh. Dtsch. Phys. Ges. **17**, 152 (1915).

[2] S. J. Barnett, Magnetization by rotation, Phys. Rev. **6**, 239 (1915).

[3] L. Zhang and Q. Niu, Angular Momentum of Phonons and the Einstein–de Haas Effect, Phys. Rev. Lett. **112**, 085503 (2014).

[4] D. A. Garanin and E. M. Chudnovsky, Angular momentum in spin-phonon processes, Phys. Rev. B **92**, 024421 (2015).

[5] C. Dornes, Y. Acremann, M. Savoini, M. Kubli, M. J. Neugebauer, E. Abreu, L. Huber, G. Lantz, C. A. F. Vaz, H. Lemke, E. M. Bothschafter, M. Porer, V. Esposito, L. Rettig, M. Buzzi, A. Alberca, Y. W. Windsor, P. Beaud, U. Staub, D. Zhu, S. Song, J. M. Glownia, and S. L. Johnson, The ultrafast Einstein–de Haas effect, Nature **565**, 209 (2019).

[6] A. Rückriegel, S. Streib, G. E. W. Bauer, and R. A. Duine, Angular momentum conservation and phonon spin in magnetic insulators, Phys. Rev. B **101**, 104402 (2020).

[7] D. A. Garanin and E. M. Chudnovsky, Conservation of angular momentum in an elastic medium with spins, Phys. Rev. B **103**, L100412 (2021).

[8] S. R. Tauchert, M. Volkov, D. Ehberger, D. Kazenwadel, M. Evers, H. Lange, A. Donges, A. Book, W. Kreuzpaintner, U. Nowak, and P. Baum, Polarized phonons carry angular momentum in ultrafast demagnetization, Nature **602**, 73 (2022).

[9] L. Zhang and Q. Niu, Chiral phonons at high-symmetry points in monolayer hexagonal lattices, Phys. Rev. Lett. **115**, 115502 (2015).

[10] M. Hamada, E. Minamitani, M. Hirayama, and S. Murakami, Phonon angular momentum induced by the temperature gradient, Phys. Rev. Lett. **121**, 175301 (2018).

[11] J. Zhong, H. Sun, Y. Pan, Z. Wang, X. Xu, L. Zhang, and J. Zhou, Abnormal phonon angular momentum due to off-diagonal elements in the density matrix induced by a temperature gradient, Phys. Rev. B **107**, 125147 (2023).

[12] H. Zhang, N. Peshcherenko, F. Yang, T. Z. Ward, P. Raghuvanshi, L. Lindsay, C. Felser, Y. Zhang, J. Q. Yan, and H. Miao, Observation of phonon angular momentum (2024), arXiv:2409.13462 [cond-mat.str-el].

[13] T. Wang, H. Sun, X. Li, and L. Zhang, Chiral phonons: Prediction, verification, and application, Nano Letters **24**, 4311 (2024).

[14] S. Streib, Difference between angular momentum and pseudoangular momentum, Phys. Rev. B **103**, L100409 (2021).

[15] S. Chaudhary, D. M. Juraschek, M. Rodriguez-Vega, and G. A. Fiete, Giant effective magnetic moments of chiral phonons from orbit-lattice coupling, Phys. Rev. B **110**, 094401 (2024).

[16] M. J. Rice and H.-Y. Choi, Charged-phonon absorption in doped c_{60}, Phys. Rev. B **45**, 10173 (1992).

[17] Y. Pak, I. Sibert, Edwin L., and R. C. Woods, Coupled cluster anharmonic force fields, spectroscopic constants, and vibrational energies of AlF_3 and SiF_3^+, The Journal of Chemical Physics **107**, 1717 (1997), https://pubs.aip.org/aip/jcp/article-pdf/107/6/1717/19218415/1717_1_online.pdf.

[18] A. Nejad and D. L. Crittenden, On the separability of large-amplitude motions in anharmonic frequency calculations, Phys. Chem. Chem. Phys. **22**, 20588 (2020).

[19] V. G. Solomonik and O. Y. Marochko, Molecular Structures and Vibrational Spectra of ScF3, YF3, and LaF3 as Calculated by the CISD+Q Method, Journal of Structural Chemistry **41**, 725 (2000).

[20] J. W. Zwanziger and E. R. Grant, Topological phase in molecular bound states: Application to the $E \times e$ system, The Journal of Chemical Physics **87**, 2954 (1987), https://pubs.aip.org/aip/jcp/article-pdf/87/5/2954/18965948/2954_1_online.pdf.

[21] P. E. Maslen, N. C. Handy, R. D. Amos, and D. Jayatilaka, Higher analytic derivatives. IV. Anharmonic effects in the benzene spectrum, The Journal of Chemical Physics **97**, 4233 (1992), https://pubs.aip.org/aip/jcp/article-pdf/97/6/4233/19001899/4233_1_online.pdf.

[22] J. Medina, F. Avilés, and A. Tapia, The bond force constants of graphene and benzene calculated by density functional theory, Molecular Physics **113**, 1297 (2015), https://doi.org/10.1080/00268976.2014.986241.

[23] M. Preuss and F. Bechstedt, Vibrational spectra of ammonia, benzene, and benzene adsorbed on Si (110) by *first principles* calculations with periodic boundary conditions, Phys. Rev. B **73**, 155413 (2006).

[24] J. E. Bertie and C. D. Keefe, Infrared intensities of liquids XXIV: optical constants of liquid benzene-h_6 at

25 °C extended to 11.5 cm^{-1} and molar polarizabilities and integrated intensities of benzene-h_6 between 6200 and 11.5 cm^{-1}, Journal of Molecular Structure **695–696**, 39 (2004), Winnewisser Special Issue.